Electronic Supplementary Material (ESI) for Nanoscale.

Electronic Supplementary Information

Synthesis and characterization of [7]triangulene

Shantanu Mishra, Kun Xu, Kristjan Eimre, Hartmut Komber, Ji Ma, Carlo A. Pignedoli, Roman Fasel, Xinliang Feng, and Pascal Ruffieux

Contents

Additional STM data and theoretical calculations Page 2

Experimental and theoretical methods including synthetic procedures and solution characterization data Page 5

References Page 14

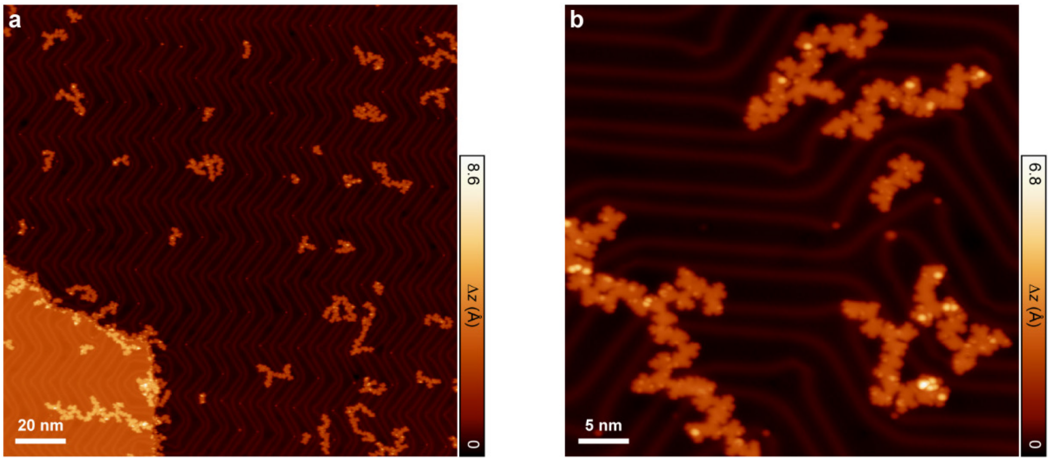

Fig. S1 Large-scale (a) and zoom-in (b) STM images after annealing precursor mixture **1**+**1'** on Au(111) at 350 °C. The surface topography is dominated by covalently coupled molecular clusters, and no isolated nanographenes are found. Scanning parameters for STM images: $V = -1.20$ V, $I = 40$ pA.

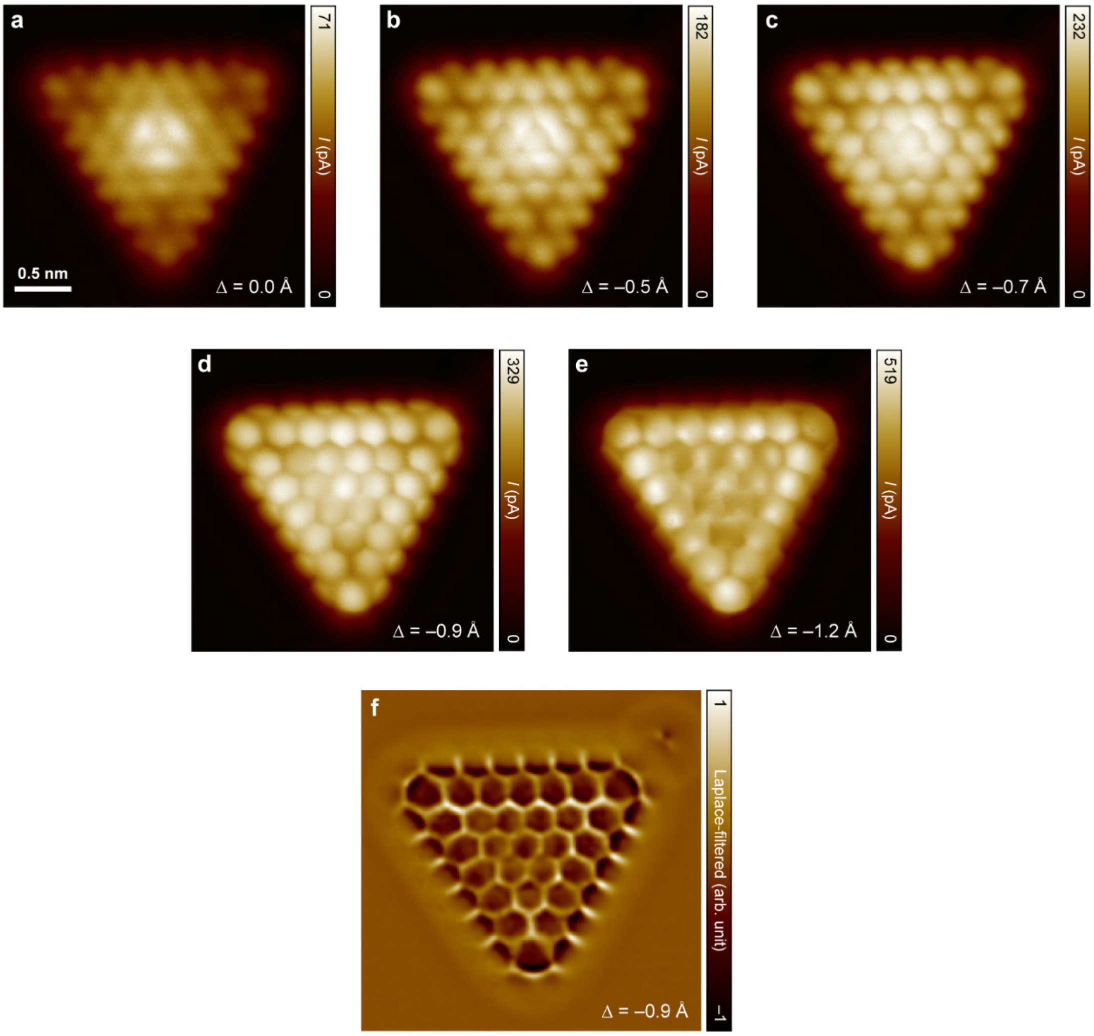

Fig. S2 (a–e) Series of ultrahigh-resolution STM images of **1** at varying Δ values. Panels (a) and (d) are shown in Fig. 1. (f) Laplace-filtered representation of (d), providing enhanced structural contrast. Open feedback parameters: $V = -5$ mV, $I = 50$ pA.

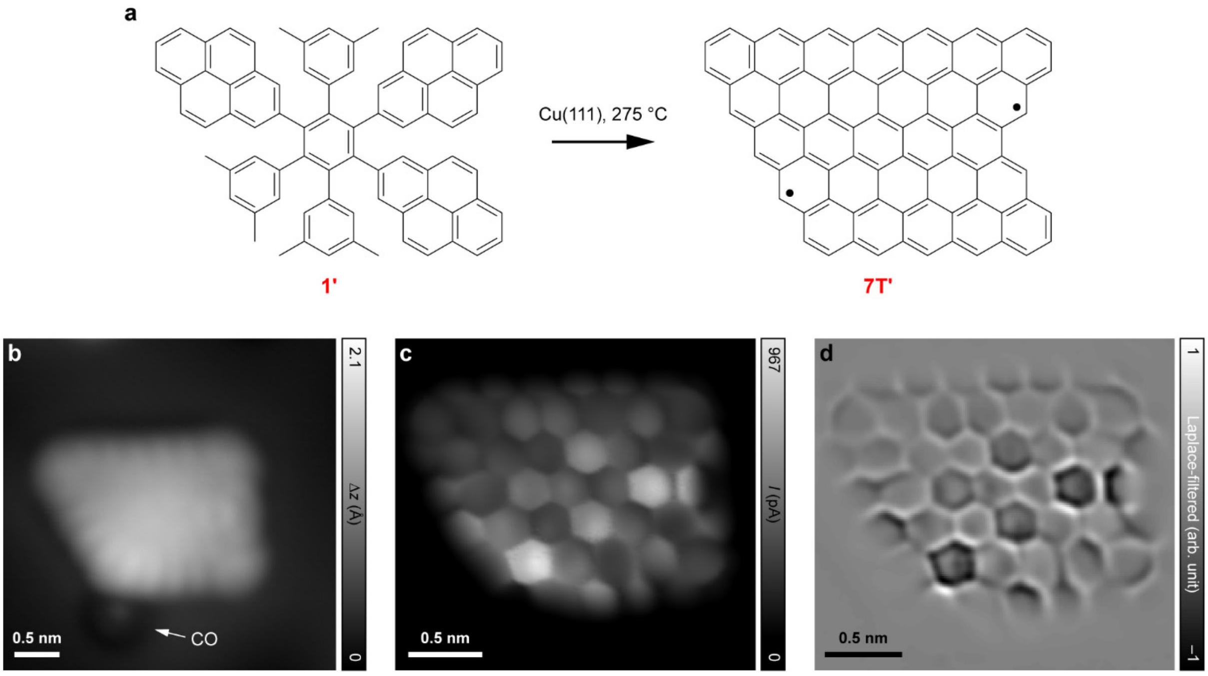

Fig. S3 (a) Schematic illustration of the formation of **7T'** from cyclodehydrogenation and oxidative cyclization reactions of **1'**. (b) High-resolution STM image of **7T'** acquired with a CO functionalized tip ($V = -0.10$ V, $I = 100$ pA). (c) Corresponding ultrahigh-resolution STM image of **7T'** ($V = -5$ mV, $I = 50$ pA; $\Delta = -0.9$ Å). (d) Laplace-filtered representation of (c).

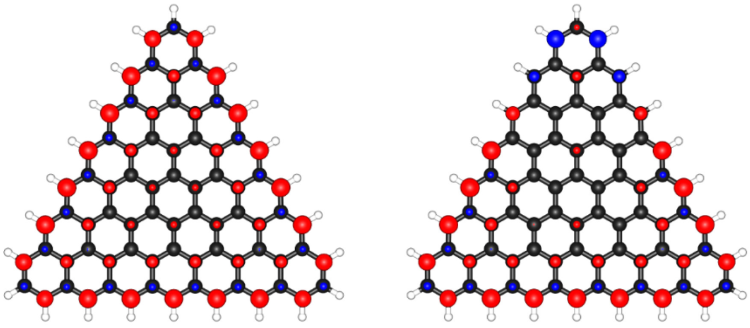

$S = 3$, 0 eV (ground state)

$S = 2$, 0.25 eV

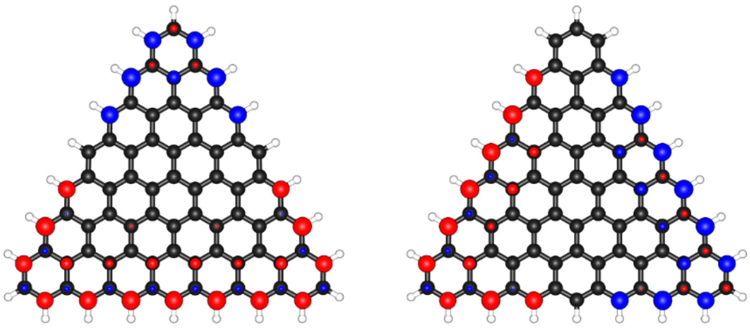

$S = 1$, 0.30 eV

$S = 0$, 0.33 eV

Fig. S4 DFT-calculated spin density isosurfaces for the $S = 0$ to $S = 3$ magnetic states of **7T** (isovalue: 0.01 a.u.; red and blue isosurfaces denote spin up and spin down densities, respectively), along with their relative energies with respect to the $S = 3$ ground state.

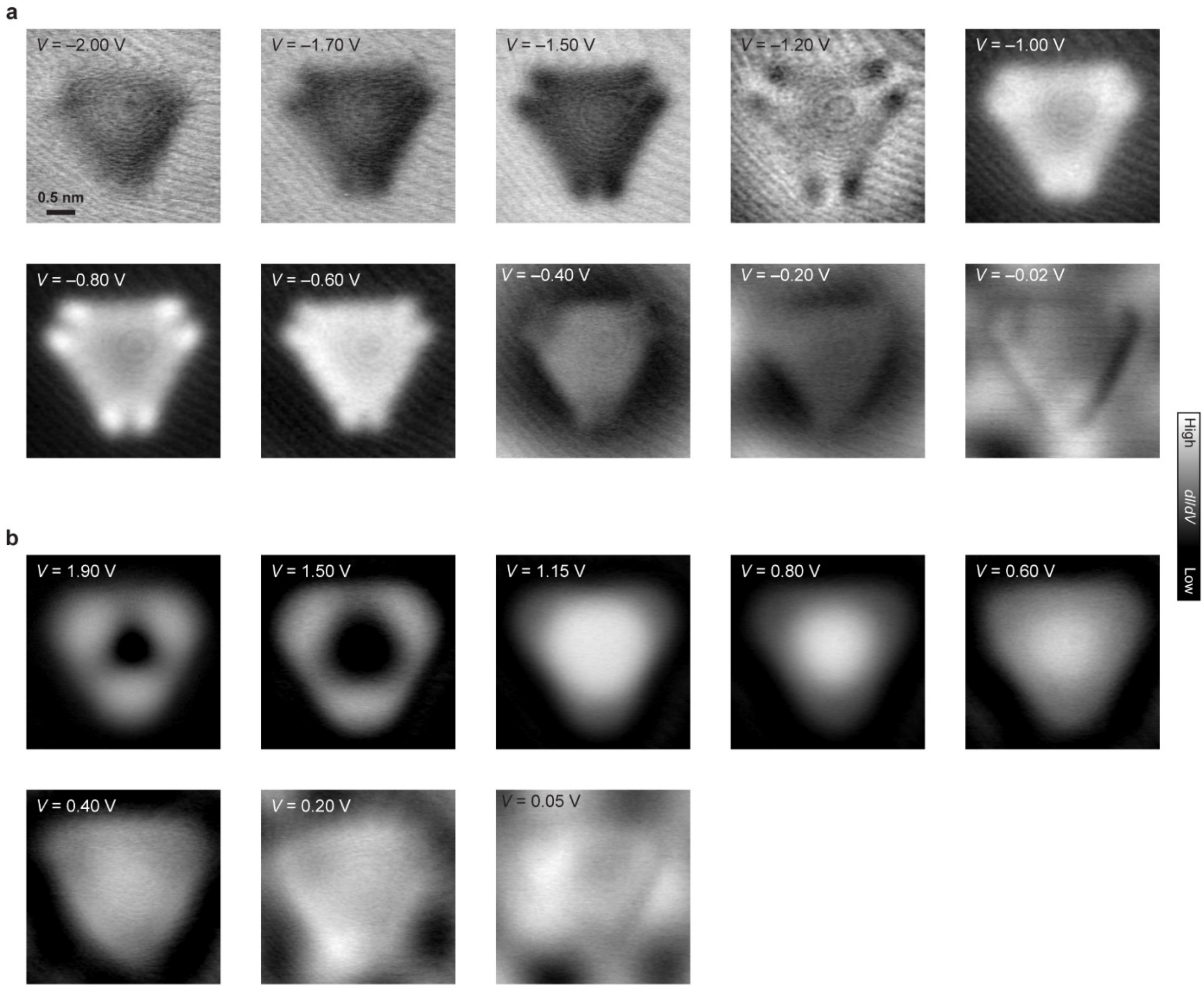

Fig. S5 Sequence of dI/dV maps acquired at negative (a) and positive (b) biases. Scanning parameters: I = 200–350 pA; V_{rms} = 10 mV (maps at –0.02 V and 0.05 V) and 22 mV (all other maps). No signatures of spin-split singly occupied MOs, appearing similar at both bias polarities, are found, indicating a closed-shell ground state of **7T** on Cu(111).

Experimental and theoretical methods

1. Sample preparation and STM/STS measurements

STM measurements were performed with a Scienta Omicron low temperature STM operating at 4.5 K and base pressure below 5×10^{-11} mbar. Au(111) and Cu(111) single crystal surfaces were prepared by Ar^+ sputtering and annealing cycles. Precursor mixture **1+1'** was contained in a quartz crucible and deposited at 610 K from a home-built evaporator on the respective surfaces held at room temperature. STM images and dI/dV maps were acquired in constant-current mode, while dI/dV spectra were acquired in constant-height mode. Unless noted otherwise, gold- or copper-coated tungsten tips were used for STM imaging and dI/dV spectroscopy. Indicated tunneling biases are provided with respect to the sample. dI/dV spectra and maps were acquired with a lock-in amplifier operating at a frequency of 860 Hz. Lock-in modulation voltages (root mean square amplitude, V_{rms}) for each measurement is provided in the respective figure captions. Ultrahigh-resolution STM images were acquired with CO functionalized tips, where the molecules are scanned in a constant-height mode and the current channel is displayed. The data shown in this study were processed and analyzed with WaveMetrics Igor Pro or WSxM[1] software.

2. Theoretical methods

The DFT calculations of **7T** on Cu(111) surface were performed with the CP2K code[2] utilizing the AiiDA-lab[3] platform. We used a TZV2P Gaussian basis set[4] for C and H species and a DZVP basis set for Cu species, together with a cutoff of 600 Ry for the plane wave basis set. Norm-conserving Goedecker-Teter-Hutter pseudopotentials[5] and the PBE exchange-correlation functional,[6] with the D3 dispersion corrections proposed by Grimme et al.[7] were used. The Cu(111) surface was modelled as a slab containing 4 atomic layers of Cu along the [111] direction and a layer of hydrogen atoms to passivate one side of the slab. The modelled periodic slab surface dimensions were 38.19×35.28 Å^2, corresponding to 240 surface units. 40 Å of vacuum was included in the simulation cell to decouple the system from its periodic replicas in the direction perpendicular to the surface. To obtain the equilibrium geometries, we kept the atomic positions of the bottom two layers of the slab fixed to the ideal bulk positions, and all other atoms were relaxed until forces were lower than 0.005 eV/Å. To obtain simulated STM images within the Tersoff-Hamann approximation,[8] we extrapolated the electronic orbitals obtained from CP2K to the vacuum region in order to correct the wrong decay in vacuum of the charge density due to the localized basis. The gas phase calculations of different magnetic states of **7T** were also performed with CP2K using a cell of molecular bounding box with 15 Å of space added in each direction and other parameters kept equivalent to the surface calculations. For each magnetic state, the geometry was separately optimized.

To characterize the charge transfer, the CP2K charge density for the whole molecule and slab system was generated with a high plane-wave cutoff of 2400 Ry for a high-precision grid. Bader's basins and the atoms in molecules (AIM) analysis[9] was performed with the Fortran program developed by Henkelman's group.[10]

3. General methods and materials

Flash column chromatography (FCC) was performed using MACHEREY-NAGEL silica gel 60® (230-400 mesh). Thin layer chromatography (TLC) was performed on aluminum plates pre-coated with silica gel (Merck, silica 60, F_{254}) or Al_2O_3 TLC-PET foils (Sigma-Aldrich), and visualized by UV fluorescence (λ_{max} = 254 nm or 365 nm). Nuclear magnetic resonance (NMR) spectra were acquired on a BRUKER Avance III 500 spectrometer (500.13 MHz and 125.77 MHz for ^{1}H and ^{13}C, respectively) using the standard pulse sequences included in the TOPSPIN 3.6 software package. The measurements were carried out at 30°C. All chemical shifts are reported in parts per million (ppm) and were measured relative to the residual solvent signal (CD_2Cl_2: $\delta(^1H)$ = 5.31 ppm, $\delta(^{13}C)$ = 53.7 ppm; $C_2D_2Cl_4$: $\delta(^1H)$ = 5.98 ppm, $\delta(^{13}C)$ = 73.7 ppm). High-resolution (HR) matrix-assisted laser desorption/ionization time-of-flight (MALDI-TOF) mass spectra (MS) were obtained in the liquid-state on Autoflex Speed MALDI-TOF from BRUKER, using *trans*-2-[3-(4-tert-butylphenyl)-2-methyl-2-propenylidene]malononitrile (DCTB) as matrix substrate. Fluorescence spectra were measured on PerkinElmer fluorescence spectrometer LS 55. Recycling gel permeation chromatography (rGPC) purification was performed on JAI HPLC LC 9110 II NEXT with fraction collector FC-3310 and GPC columns 2H and 1H (connected in series). rGPC was used with HPLC-grade chloroform at room temperature.

Solvents: Anhydrous solvents (Et_3N, THF, Dioxane) were purchased from Sigma-Aldrich and degassed with Argon before use. Solvents employed for work-up and column chromatography were purchased in HPLC quality and used directly without further purification.

Catalysts and ligands: catalysts, ligands and silver salts were purchased from Sigma-Aldrich or Strem and used without further purification.

4. Synthetic procedures

Synthesis of isomeric mixture of 2,2',2''-(5'-(3,5-dimethylphenyl)-3,3'',5,5''-tetramethyl-[1,1':3',1''-terphenyl]-2',4',6'-triyl)tripyrene (**1**) and 2,2',2''-(5'-(3,5-dimethylphenyl)-3,3'',5,5''-tetramethyl-[1,1':2',1''-terphenyl]-3',4',6'-triyl)tripyrene (**1'**).

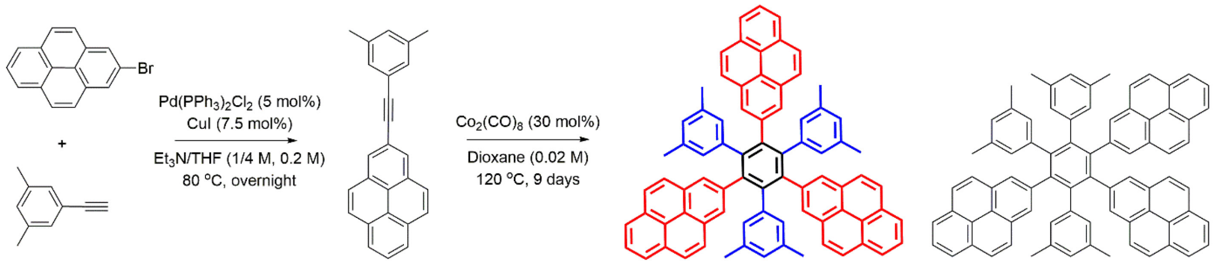

2 **1** **1'**

Synthesis of 2. To a Schlenk tube was added 2-bromopyrene[11] (1.10 g, 3.92 mmol, 1.0 equiv), 1-ethynyl-3,5-dimethylbenzene[12] (510 mg, 3.92 mmol, 1.0 equiv), $Pd(PPh_3)_4$ (137.5 mg, 0.196 mmol, 5 mol%), CuI (55.9 mg, 0.294 mmol, 7.5 mol%), Et_3N (4.0 mL) and THF (16 mL). The reaction mixture was heated at 80 °C overnight. After cooling down to room temperature, all volatiles were removed by rotary evaporation. The resulting residue was then purified by FCC with silica gel (isohexane, R_f = 0.18), and then rGPC to afford desired product as a white solid (**2**, 600.0 mg, 46%).

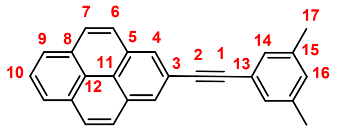

^{1}H NMR (500 MHz, CD_2Cl_2) δ = 8.34 (s, 2H; 4), 8.22 (d, J = 7.6 Hz, 2H; 9), 8.13 (d, J = 9.0 Hz, 2H; 7), 8.07 (d, J = 9.0 Hz, 2H; 6), 8.05 (t, J = 7.6 Hz, 1H; 10), 7.30 (m, 2H; 14), 7.06 (m, 1H; 16), 2.37 (s, 6H; 17).

^{13}C NMR (125 MHz, CD_2Cl_2) δ = 138.5 (15), 131.6 (8), 131.5 (5), 130.7 (16), 129.6 (14), 128.4 (7), 127.9 (4), 127.2 (6), 126.7 (10), 125.7 (9), 124.6 (12), 124.4 (11), 123.1 (3 or 13), 121.2 (3 or 13), 90.5 (1), 89.4 (2), 21.2 (17).

HR MALDI-TOF MS (*m/z*): [M] calcd for $C_{26}H_{18}$: 330.1409, found: 330.1411 (error: 0.6 ppm).

Synthesis of 1 and 1'. To a Schlenk tube was added precursor **2** (198.0 mg, 0.6 mmol, 1.0 equiv), $Co_2(CO)_8$ (61.6 mg, 0.18 mmol, 30 mol%) and dioxane (30 mL). The resulting mixture was heated at 120 °C for 9 days. After cooling down to room temperature, all volatiles were removed via rotary evaporation. The resulting residue was purified by FCC (dichloromethane/isohexane = 1/2, R_f = 0.37) to afford a major fraction as a white solid (**A**, 74 mg); and a minor, yellowish fraction with unidentified impurities. The minor fraction was then followed by rGPC purification to afford a white solid (**B**, 36 mg); total yield: 55%. NMR analysis indicated that fraction **A** and **B** contain different ratios of **1** and **1'**.

*Comment on NMR analysis: The reaction product was studied as mixture of **1** and **1'**. No hindered rotation of pyrene or 3,5-dimethylphenyl moieties was observed at 30°C. In the ^{1}H NMR spectrum of this mixture, only the signals of the 3,5-dimethylphenyl moieties could be assigned for **1** and **1'**. The signals of the pyrene residues overlap in the narrow 8.1-7.7 ppm region preventing a signal assignment for **1'**. The values reported for **1** were determined from the HSQC spectrum. The symmetric isomer **1** results in seventeen assigned ^{13}C signals. For non-symmetric isomer **1'**, three times the number of signals is expected. In fact, three signals were observed for several positions (1, 2, 3, 12, 13, 17), for* *other positions signals overlap. The compilation of ^{13}C NMR data reports for **1'** regions where the signals of an atom position occur.*

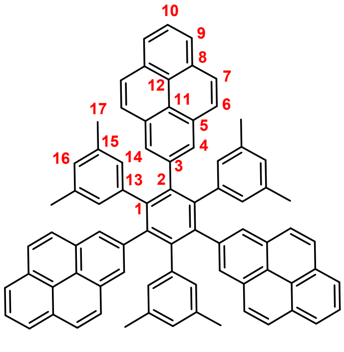

1

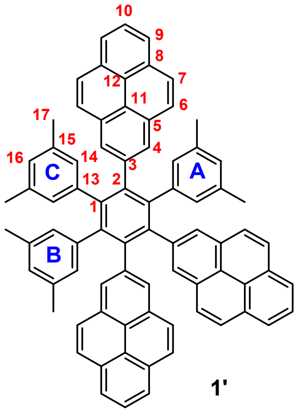

1'

^{1}**H NMR** (500 MHz, $C_2D_2Cl_4$): Isomer **1** - δ = 8.06 (d, *J* = 7.6 Hz, 6H; 9), 8.00 (s, 6H; 4), 7.90 (t, *J* = 7.6 Hz, 3H; 10), 7.89 (d, *J* = 9.1 Hz, 6H; 7), 7.84 (d, *J* = 9.1 Hz, 6H; 6), 6.80 (s, 6H; 14), 5.96 (s, 3H; 16), 1.68 (s, 18H; 17); isomer **1'** – δ = 8.5-7.7 (27H; all pyrene protons), 6.78 (s, 4H; 14), 6.76 (s, 2H; 14), 6.22 (s, 1H; 16B/C), 6.19 (s, 1H; 16 B/C), 5.93 (s, 1H; 16A), 1.87 (s, 6H; 17B/C), 1.84 (s, 6H; 17B/C), 1.65 (s, 6H; 17A).

^{13}**C NMR** (125 MHz, $C_2D_2Cl_4$): Isomer **1** - δ = 141.1 (1), 139.8 (2 or 3), 139.5 (2 or 3), 138.7 (13), 135.0 (15), 130.6 (8), 129.1 (5), 128.8 (14), 128.3 (4), 127.5 (6), 126.2 (7 and 16), 125.3 (10), 124.3 (9), 124.0 (12), 122.1 (11), 20.6 (17); isomer **1'** – δ = 140.9, 140.8, 140.6 (all 1), 140.1, 140.0, 139.9, 139.85, 139.8, 139.75 (all 2 or 3), 138.9, 138.6, 138.5 (all 13), 135.2-134.8 (15), 130.7-130.5 (8), 129.1 (5), 129.0 and 128.8 (14), 128.3 and 128.1 (4), 127.4 and 127.2 (6), 126.4-126.0 (7 and 16), 125.3 and 125.1 (10), 124.3 and 124.1 (9), 124.0, 123.9, 123.85 (all 12), 122.1 and 122.0 (11), 20.7, 20.65, 20.5 (all 17).

HR MALDI-TOF MS (*m/z*): [M] calcd for $C_{78}H_{54}$: 990.4226, found: 990.4202 (error: −2.4 ppm).

5. HR MALDI-TOF mass spectrometry

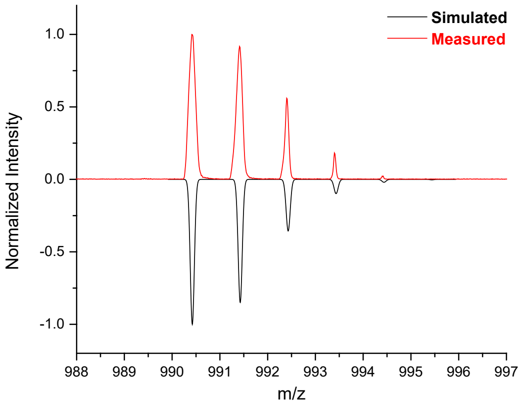

Fig. S6 HR MALDI-TOF MS of **1** and **1'**.

6. NMR characterization

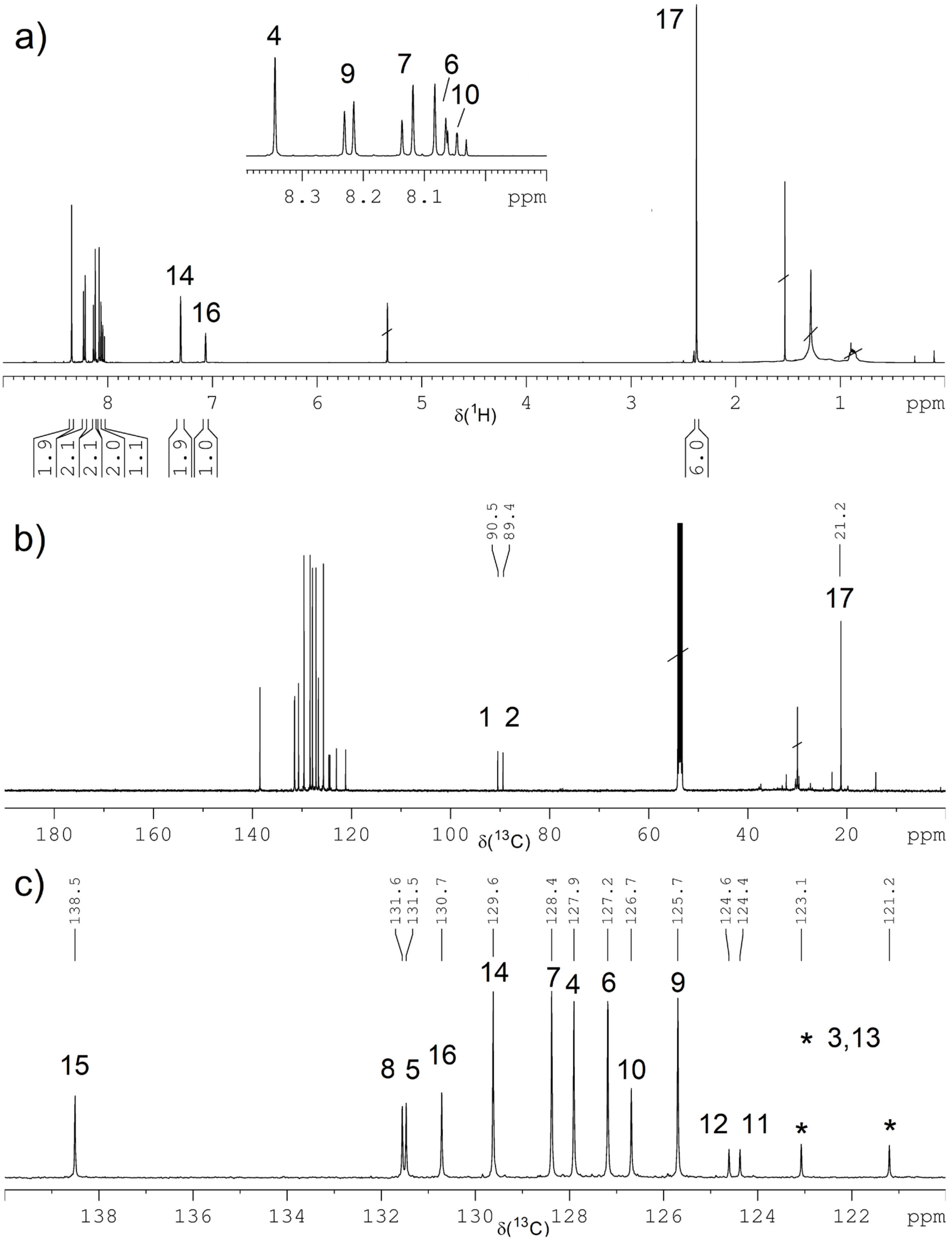

Fig. S7 ^{1}H (a) and ^{13}C NMR spectrum (b, overview; c, aromatic carbons region) of **2** (solvent: CD_2Cl_2).

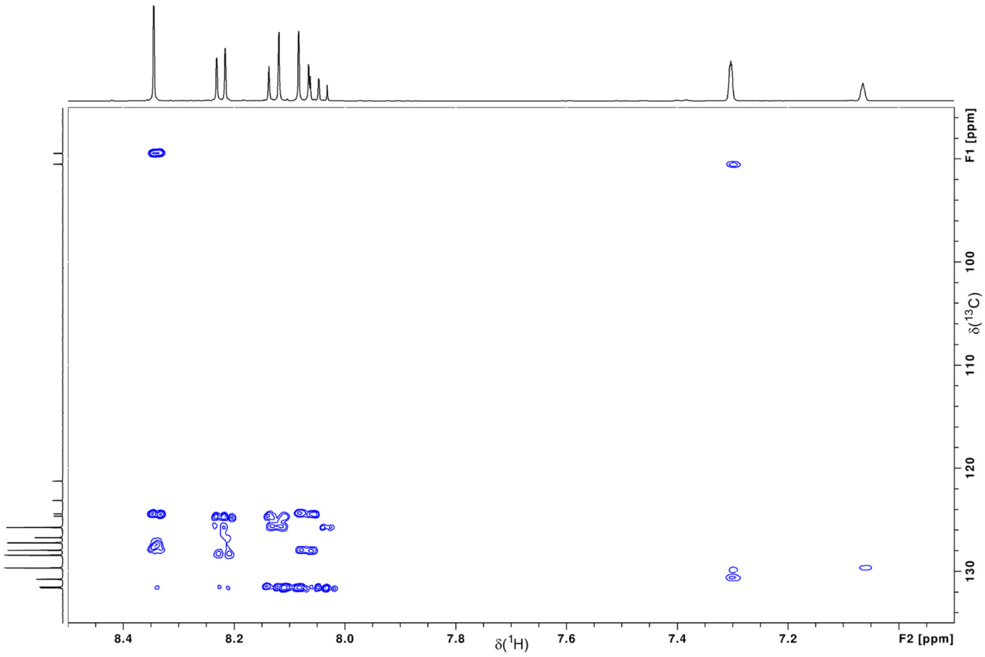

Fig. S8 HMBC spectrum (region) of **2** (solvent: CD_2Cl_2).

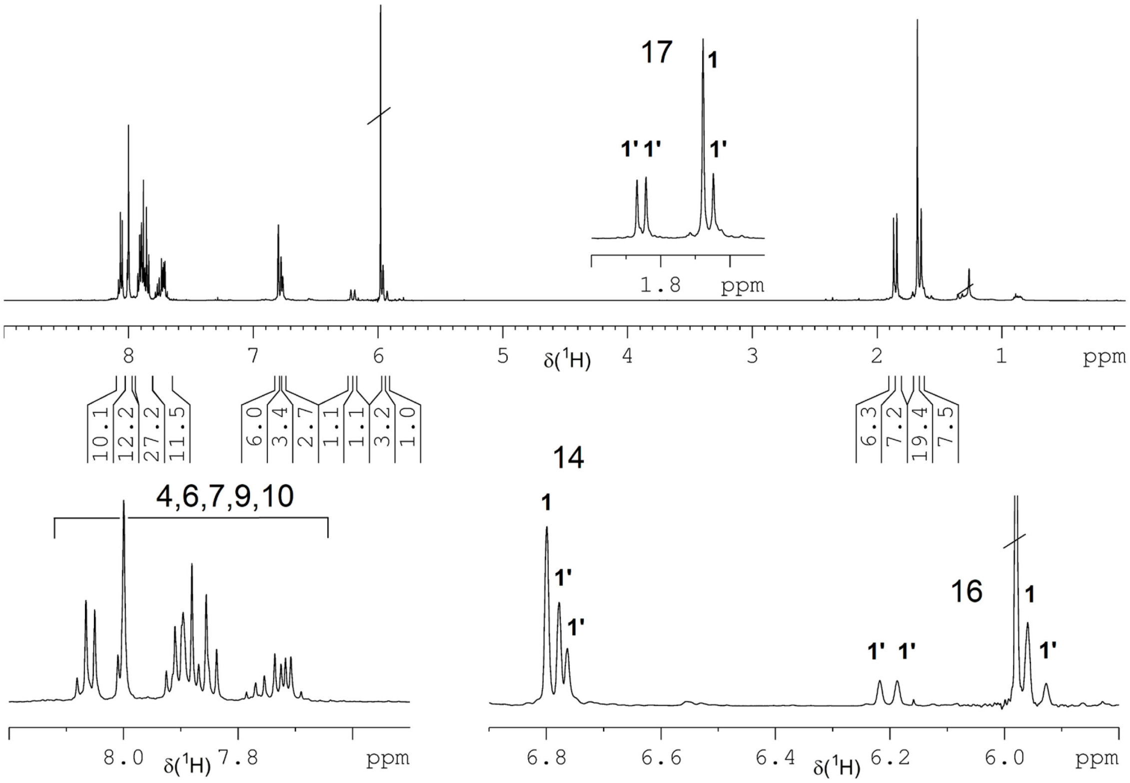

Fig. S9 ^{1}H NMR spectrum (overview and enlarged regions) of **1** and **1'** (solvent: $C_2D_2Cl_4$).

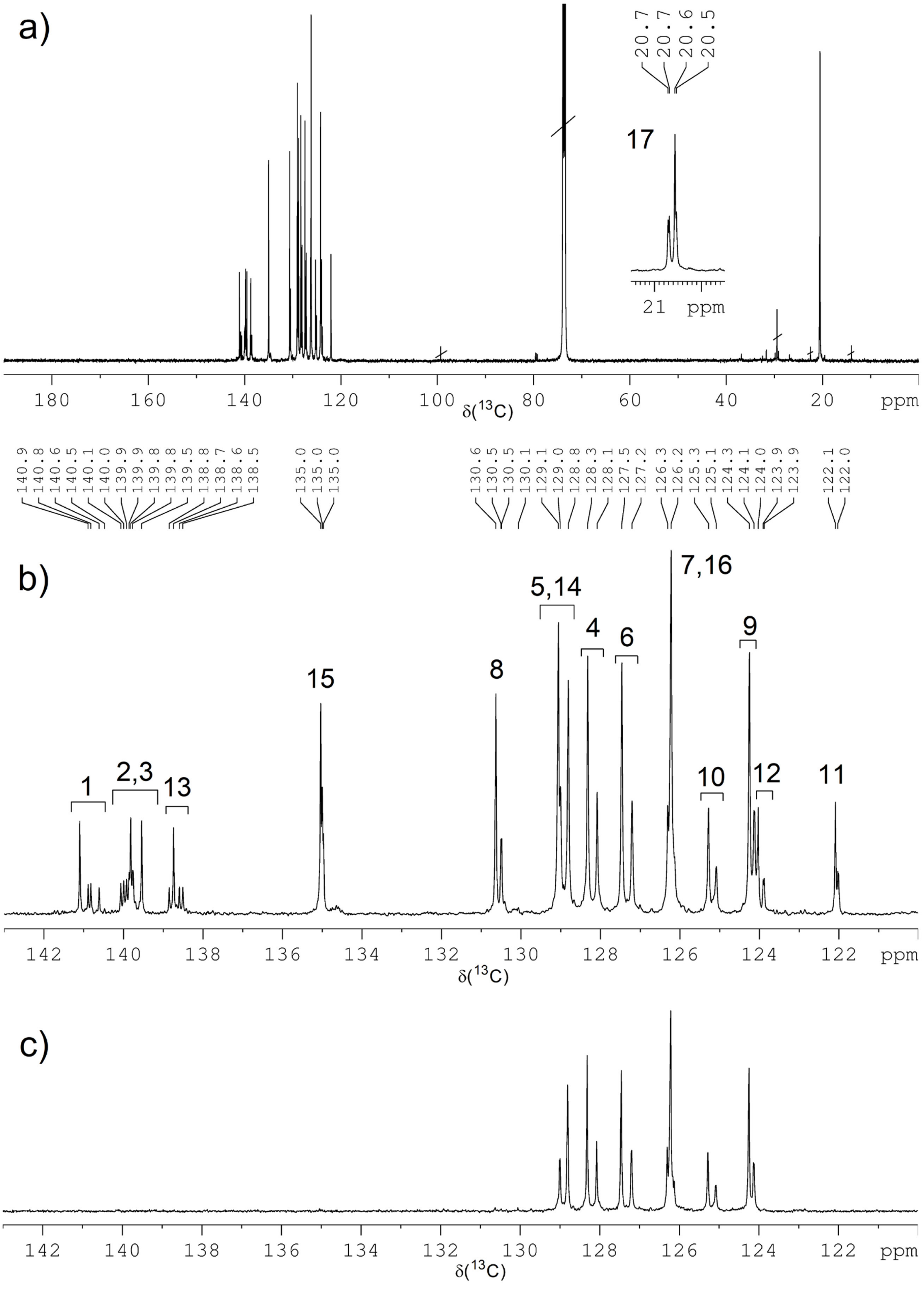

Fig. S10 ^{13}C NMR spectrum (a, overview; b, aromatic carbons' region) and DEPT135 spectrum (c) of **1** and **1'** (solvent: $C_2D_2Cl_4$).

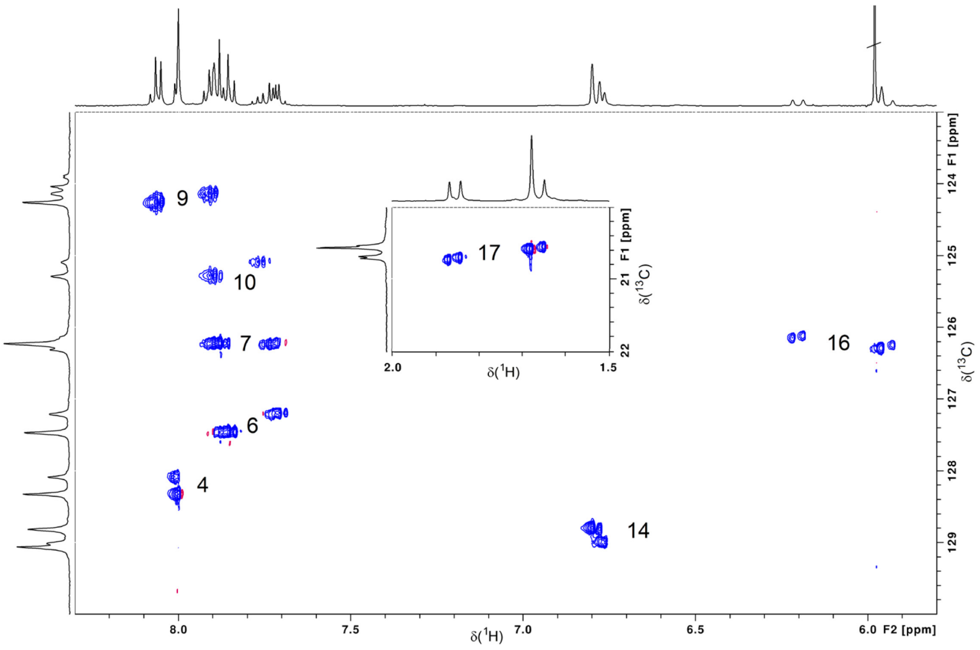

Fig. S11 HSQC spectrum (regions) of **1** and **1'** (solvent: $C_2D_2Cl_4$).

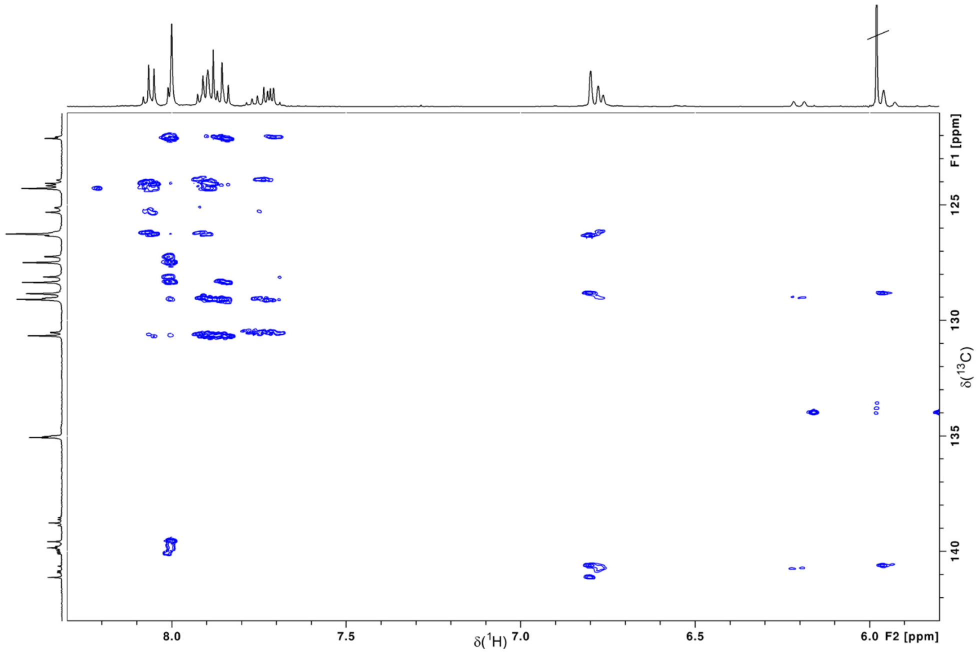

Fig. S12 HMBC spectrum (region) of **1** and **1'** (solvent: $C_2D_2Cl_4$).

References

1 I. Horcas, R. Fernández, J. M. Gómez-Rodríguez, J. Colchero, J. Gómez-Herrero and A. M. Baro, *Rev. Sci. Instrum.*, 2007, **78**, 013705.

2 J. Hutter, M. Iannuzzi, F. Schiffmann and J. VandeVondele, *Wiley Interdiscip. Rev. Comput. Mol. Sci.*, 2014, **4**, 15–25.

3 A. V. Yakutovich, K. Eimre, O. Schütt, L. Talirz, C. S. Adorf, C. W. Andersen, E. Ditler, D. Du, D. Passerone, B. Smit, N. Marzari, G. Pizzi and C. A. Pignedoli, *Comput. Mater. Sci.*, 2021, **188**, 110165.

4 J. VandeVondele and J. Hutter, *J. Chem. Phys.*, 2007, **127**, 114105.

5 S. Goedecker, M. Teter and J. Hutter, *Phys. Rev. B*, 1996, **54**, 1703–1710.

6 J. P. Perdew, K. Burke and M. Ernzerhof, *Phys. Rev. Lett.*, 1996, **77**, 3865–3868.

7 S. Grimme, J. Antony, S. Ehrlich and H. Krieg, *J. Chem. Phys.*, 2010, **132**, 154104.

8 J. D. Tersoff and D. R. Hamann, *Phys. Rev. B*, 1985, **31**, 805–813.

9 R. F. W. Bader, *Atoms in Molecules: A Quantum Theory*, Oxford University Press, Oxford, 1994.

10 W. Tang, E. Sanville and G. Henkelman, *J. Phys.: Condens. Matter*, 2009, **21**, 084204.

11 A. G. Crawford, Z. Liu, I. A. I. Mkhalid, M.-H. Thibault, N. Schwarz, G. Alcaraz, A. Steffen, J. C. Collings, A. S. Batsanov, J. A. K. Howard and T. B. Marder, *Chem. Eur. J*, 2012, **18**, 5022–5035.

12 W. Zhao, L. Huang, Y. Guan and W. D. Wulff, *Angew. Chem. Int. Ed.*, 2014, **53**, 3436–3441.